

# Quantitative Analysis of NKX2-3 Expression in Human Colon: An Immunohistochemical Study

Fanni Gábris , Béla Kajtár , Zoltán Kellermayer, and Péter Balogh 

Department of Immunology and Biotechnology (FG, ZK, PB) and Department of Pathology (BK), Medical School, University of Pécs, Pécs, Hungary, and Lymphoid Organogenesis Research Team, Szentágotthai Research Centre, University of Pécs, Pécs, Hungary (FG, ZK, PB)

## Summary

In mice, Nkx2-3 homeodomain transcription factor defines the vascular specification of secondary and tertiary lymphoid tissues of the intestines. In human studies, polymorphisms in NKX2-3 have been identified as a susceptibility factor in inflammatory bowel diseases, whereas in mice, its absence is associated with protection against experimental colitis and enhanced intestinal epithelial proliferation. Here, we investigated the expression of NKX2-3 in normal, polyp, and adenocarcinoma human colon samples using immunohistochemistry and quantitative morphometry, correlating its expression with endothelial and mesenchymal stromal markers. Our results revealed that the expression of NKX2-3 is regionally confined to the lamina propria and lamina muscularis mucosae, and its production is restricted mostly to endothelial cells and smooth muscle cells with variable co-expression of CD34, alpha smooth muscle antigen ( $\alpha$ SMA), and vascular adhesion protein-1 (VAP-1). The frequency of NKX2-3-positive cells and intensity of expression correlated inversely with aging. Furthermore, in most colorectal carcinoma samples, we observed a significant reduction of NKX2-3 expression. These findings indicate that the NKX2-3 transcription factor is produced by both endothelial and non-endothelial tissue constituents in the colon, and its expression changes during aging and in colorectal malignancies. (J Histochem Cytochem 72: 11–23, 2024)

## Keywords

adenocarcinoma, colon, endothelium, NKX2-3, polyp, stroma

## Introduction

The gut performs an extensive array of vital biological functions, including digestion, nutrient absorption, mucus secretion, fluid homeostasis, and immunological defense of the intestines. This functional complexity requires a highly organized tissue architecture, via integrating divergent epithelial components, smooth muscle layers, lymphatic and blood vasculature, autonomous innervation, and mucosal lymphoid tissues that can also maintain tissue integrity and a balanced intestinal microbiome composition.<sup>1–4</sup>

The synchronized development of the gut involves the differentiation of several types of cells with diverse origins. Epithelial cells develop from the endoderm

and, following embryonic specialization, undergo continuous renewal and specification from Lgr5<sup>+</sup> epithelial stem cells, located at the bottom of intestinal crypts.<sup>5,6</sup> The muscle layers and other mesenchymal elements providing tissue organization and contractility develop from the splanchnic region of the lateral plate mesoderm under the influence of Hedgehog signaling emanating from the epithelium,<sup>7–9</sup> while the autonomous

Received for publication August 23, 2023; accepted November 6, 2023.

## Corresponding Author:

Péter Balogh, Department of Immunology and Biotechnology, Medical School, University of Pécs, Szegedi út 12, 7624 Pécs, Hungary.

E-mail: balogh.peter@pte.hu

neural elements originate from the vagal and sacral neural crest-derived progenitors, organized into the submucosal and myenteric plexuses.<sup>10,11</sup> These neuronal components (including glial cells) interact with intestinal lymphoid tissues.<sup>12</sup> Of these, the programmed lymphoid tissues (such as the Peyer's patches [PPs] in the small intestine and colonic patches in the colon, respectively) develop before birth, while the microbe-induced transformation of colonic cryptopatches (CPs) into isolated lymphoid follicles (ILFs) takes place postnatally.<sup>13–15</sup> In the human intestines, altogether over 100 different types of cellular components have been identified from various anatomical locations along the gut using high-throughput single-cell RNA sequencing (scRNAseq).<sup>16–18</sup>

Several transcription factors regulating gut development belong to the homeodomain-containing transcription factor families.<sup>19,20</sup> In a complex lineage-, cell-type, and context-dependent fashion, these transcription factors act in a temporal and spatial pattern. Of these, the Nkx family members create an “Nkx code” that can be linked to various organ-specific developmental processes, and they also participate in various malignancies.<sup>21,22</sup> As an important regulator, Nkx2-1 has been identified to influence rearranged during transfection (RET) expression in enteric neural cells,<sup>23</sup> whereas Nkx2-3 acts as a critical mediator promoting intestinal vascular patterning,<sup>24–26</sup> also influencing PP high-endothelial-venule (HEV) vascular addressin specification and gut lymphocyte homeostasis.<sup>27,28</sup> Lack of Nkx2-3 confers protection from colitis in a chemically induced mouse model.<sup>29</sup> Furthermore, Nkx2-3<sup>+</sup> pericryptal mesenchymal cells may also contribute to the colonic epithelial stem cell niche, potentially influencing colonic cancer progression.<sup>30</sup>

The expression pattern of Nkx2-3 mRNA has been previously characterized in murine embryos,<sup>31</sup> and earlier immunohistochemical data in human samples suggested a restricted display of NKX2-3 in colonic lamina propria mesenchymal cells.<sup>22</sup> However, the colonic expression pattern of NKX2-3 protein has not been thoroughly investigated yet. In the present work, we report the postnatal and age-associated expression pattern in healthy human colon, as well as in colorectal polyp and carcinoma (CRC) samples. We also extend previous immunohistochemical analyses using dual labeling for endothelial, smooth muscle, and myofibroblast markers, which reveal a shared non-epithelial/non-leukocytic expression of NKX2-3 in a regionally restricted manner, but without clear identifiable lineage affiliation.

## Materials and Methods

### Criteria for Sample Selection

Sample materials were selected from the diagnostic tissue archive of the Department of Pathology, Clinical Center of the University of Pécs. For the studies, we established five categories, including (A) healthy neonates and infants (0–3 years, average age 1.3 years,  $n=10$ ); (B) healthy adolescents (15–20 years, average age 17.9 years,  $n=5$ ); (C) healthy adults and seniors (50–80 years, average age 65.8 years,  $n=10$ ); (D) patients with colonic polyps (46–73 years, average age 62.5 years,  $n=10$ ); and (E) patients with CRC (63–88 years, average age 71.7 years,  $n=15$ ; detailed in Table 1). Tissue samples were considered healthy if they were devoid of malignant, hypoxic/necrotic, or inflammatory lesions, examined by experienced pathologists. The histopathological diagnosis of polyp samples was adenomatous polyp with low-grade dysplasia, while all tumors were adenocarcinomas (Table 1). The ethical permit under the license number 8578-PTE 2020 was issued by the Regional Research Ethical Committee of the University of Pécs Clinical Center.

### Antibodies and Reagents

We used the following primary antibodies: anti-NKX2-3 (clone #5GAL454C) as a hybridoma supernatant,<sup>32</sup> anti-CD34 (clone QBend 10, DAKO), anti-alpha smooth muscle actin ( $\alpha$ SMA, clone 1A4, DAKO), anti-CD45 (clones 2B11+PD7/26, DAKO), and anti-vascular adhesion protein (anti-VAP)/AOC3 (VAP-1, clone 393112, R&D). As secondary antibodies, ImmPRESS horse-radish peroxidase (HRP)-conjugated goat anti-rat IgG (mouse absorbed) antibody (Vector Laboratories) and BondTM Polymer Refine Red Detection kit were used.

### Immunohistochemistry

Tissue sections at 4- $\mu$ m thickness were cut from 4% buffered formaldehyde-fixed and paraffin-embedded blocks with a microtome and placed on positively charged superfrost plus adhesion slides (Epredia; TS Labor, Budapest, Hungary). Deparaffinization and antigen retrieval were performed using DAKO PT Link Pre-Treatment Modul with DAKO EnVision FLEX Target Retrieval Solution, High pH (50 $\times$ ) reagent, and sections were heated for 20 minutes at 97°C followed by cooling to 65°C. Blocking and quenching of endogenous peroxidase activity were performed with an EnVision FLEX Peroxidase-Blocking Reagent for 10

**Table 1.** Characteristics of Samples Used: Age, Site of Sample, Type of Sample, and Histological Diagnosis.

	Age (Years)	Sample Location	Sample Type	Diagnosis
Normal neonates/infants	0.3	Rectum	Biopsy	Colon atresia
	0.1	Rectum	Excision	Intact rectum
	0.1	Rectum	Biopsy	Hirschsprung's disease
	2.7	Rectum	Excision	Hirschsprung's disease
	2.2	Sigmoid colon	Biopsy	Hirschsprung's disease
	0.4	Descending colon	Biopsy	Intact colon
	3.4	Rectum	Excision	Intact rectum
	0.1	Rectum	Biopsy	Hirschsprung's disease
	3.3	Rectum	Biopsy	Hirschsprung's disease
	0.1	Rectum	Excision	Intact rectum
Normal adolescents	18.2	Sigmoid colon	Biopsy	Intact colon
	19.2	Sigmoid colon/rectum	Biopsy	Intact colon
	16.3	Sigmoid colon	Biopsy	Intact colon
	18.0	Sigmoid colon	Biopsy	Intact colon
	17.7	Colon cascade (rectum)	Biopsy	Intact colon
Normal adults and seniors	58.9	Descending colon	Polypectomy	Intact colon
	59.3	Sigmoid colon	Polypectomy	Intact colon
	60.6	Sigmoid colon	Biopsy	Intact colon
	65.3	Sigmoid colon	Polypectomy	Intact colon
	65.7	Sigmoid colon	Surgical	Intact colon
	65.9	Rectum	Polypectomy	Intact colon
	68.8	Sigmoid colon	Polypectomy	Intact colon
	69.8	Ascending colon	Biopsy	Intact colon
	71.7	Sigmoid colon	Polypectomy	Intact colon
	72.4	Sigmoid colon	Surgical	Intact colon
Polyp	50.4	Sigmoid colon	Biopsy	Adenomatous polyp
	68.8	Transverse colon	Biopsy	Adenomatous polyp
	62.2	Descending colon	Biopsy	Adenomatous polyp
	56.3	Sigmoid colon	Biopsy	Adenomatous polyp
	61.6	Cecum	Biopsy	Adenomatous polyp
	71.7	Ascending colon	Biopsy	Adenomatous polyp
	63.4	Sigmoid colon	Biopsy	Adenomatous polyp
	71.7	Rectum	Biopsy	Adenomatous polyp
	73.0	Ascending colon	Biopsy	Adenomatous polyp
	45.9	Rectum	Biopsy	Adenomatous polyp
Colorectal carcinoma	65.7	Sigmoid colon	Surgical	Adenocc, LG
	72.4	Sigmoid colon	Surgical	Adenocc, HG
	72.6	Ascending colon	Surgical	Adenocc, HG
	79.0	Cecum	Surgical	Adenocc, HG
	64.2	Ascending colon	Surgical	Adenocc, LG
	86.3	Ascending colon	Biopsy	Adenocc, LG
	68.8	Sigmoid colon	Biopsy	Adenocc, LG
	63.4	Rectum	Biopsy	Adenocc, LG
	64.4	Rectum	Biopsy	Adenocc, LG
	63.6	Descending colon	Biopsy	Adenocc, LG
	87.8	Descending colon	Biopsy	Adenocc, HG
	79.4	Rectum	Biopsy	Adenocc, LG
	66.2	Rectum	Biopsy	Adenocc, LG
	62.9	Rectum	Biopsy	Adenocc, LG
	78.6	Transverse colon	Biopsy	Adenocc, LG

Abbreviations: Adenocc, adenocarcinoma; HG, high grade; LG, low grade.

minutes followed by washing with DAKO washing buffer for  $3 \times 5$  minutes. Sections were processed using DAKO Autostainer Link 48 and Leica BOND MAX stainer instruments. For single-color labeling, sections were incubated with anti-human NKX2-3 mAb for 1 hour at room temperature and washed, followed by incubation with a goat anti-rat IgG-HRP conjugate. Reactions were visualized using  $H_2O_2$ /diaminobenzidine (DAB, DAKO, EnVision FLEX Substrate buffer, EnVision FLEX DAB+Chromogen). For dual labeling, sections were next incubated with anti-human mAbs for 15 minutes. Reactions were detected with Bond Polymer Refine Red Detection kit according to Bond protocol. Nuclei were counterstained with Mayer's hematoxylin.

### Digital Image Analysis

Sections were scanned using a Panoramic Midi scanner (3D Histech Ltd, Budapest, Hungary) and were then analyzed using the QuPath-v0.2.3. software. In the lamina propria layer of sections, we randomly chose five different representative regions containing approximately 150–200 nucleated cells, counted automatically by the software. Cells were assigned into four groups based on their nuclear DAB staining optical density (OD)—negative: DAB OD mean  $<0.2$ ; weakly positive: DAB OD mean  $0.2$ – $0.4$ ; moderately positive: DAB OD mean  $0.4$ – $0.6$ ; strongly positive: DAB OD mean  $>0.6$ . During analysis, all nuclei were counted and grouped according to their labeling intensities. For the analysis of dual immunohistochemistry samples, the red, brown, and blue reaction products were digitally separated with color deconvolution of the RGB images, followed by the manual counting of cells. Samples were also evaluated according to their histoscore (H-score) feature, calculated as  $H\text{-score} = 1 \times \% \text{ weak} + 2 \times \% \text{ moderate} + 3 \times \% \text{ strong nuclei}$ , with values ranging between 0 and 300.

### Statistical Analysis

The statistical analysis of samples was performed using GraphPad Prism9. Statistical significance was determined using Mann-Whitney U-tests or Fisher's exact test. ns,  $p > 0.05$ ; \*,  $p < 0.05$ ; \*\*,  $p < 0.01$ ; \*\*\*,  $p < 0.001$ ; \*\*\*\*,  $p < 0.0001$ .

## Results

### Distribution and Ratio of NKX2-3<sup>+</sup> Cells in Healthy Human Colon

First, we investigated the expression of NKX2-3 by analyzing normal human colon tissues with

immunohistochemistry. We considered the biopsy samples normal if no inflammatory, necrotic, or neoplastic features were present. The majority of cells with nuclear NKX2-3 staining were located in the tunica mucosa and, to a lesser degree, also in the tunica muscularis, while the nuclei of epithelial cells were consistently negative for NKX2-3 (Fig. 1A–C).

As pericryptal NKX2-3<sup>+</sup> cells have been shown to influence the intestinal stem cell niche,<sup>30</sup> in our subsequent studies, we focused on analyzing the NKX2-3-positive cells within the lamina propria. Here we found that the NKX2-3<sup>+</sup> nuclei were homogeneously dispersed along the crypts (Fig. 1A and B). Next, we quantified the presence and the distribution of NKX2-3-positive cells at various ages. We found that within the lamina propria, the frequency of NKX2-3-positive nuclei was highest in the 0–3 years age group (Fig. 1D and G) and was significantly lower in both the 15–20 years age group and 50–80 years age group (Fig. 1E–G;  $p = 0.0127$  and  $p = 0.0039$ , respectively). The frequency of NKX2-3-positive cells did not differ significantly between the 15–20 years and 50–80 years age groups (Fig. 1G).

The immunohistological stainings revealed various nuclear NKX2-3 labeling intensities. Therefore, we quantified the percentage of NKX2-3-positive cells with weak, moderate, or strong expression (described in detail in the Materials and Methods section and demonstrated in Fig. 2A) and compared the frequency (defined as percentage of counted NKX2-3<sup>+</sup> lamina propria nuclei) of various labeling intensities between different age groups. In general, we observed an overall dominance of strongly positive nuclei in each age group (Fig. 2B), although the higher percentage of strong NKX2-3-expressing cells reached statistical significance only among the 15–20 years age group ( $p = 0.0079$  compared to moderate and  $p = 0.0079$  compared to weak intensities, respectively).

As a measure of overall NKX2-3 presence, we calculated the H-score which combines the frequency of NKX2-3<sup>+</sup> cells with the intensity of nuclear NKX2-3 expression. We observed a significantly higher H-score in the 0–3 age group than in the 50–80 years group ( $p = 0.0185$ , Fig. 2C). Collectively, these findings confirm our previous results on the reproducible immunohistochemical detectability of NKX2-3 protein in human biopsy samples<sup>22</sup> in the tunica mucosa and tunica muscularis layers, also revealing the dominance of strong labeling in all age groups, with the highest frequency and H-score in the 0–3 years age group.

### Characterization of NKX2-3<sup>+</sup> Cells

Due to the dispersed pattern of labeling described earlier, we assumed that several cell types express

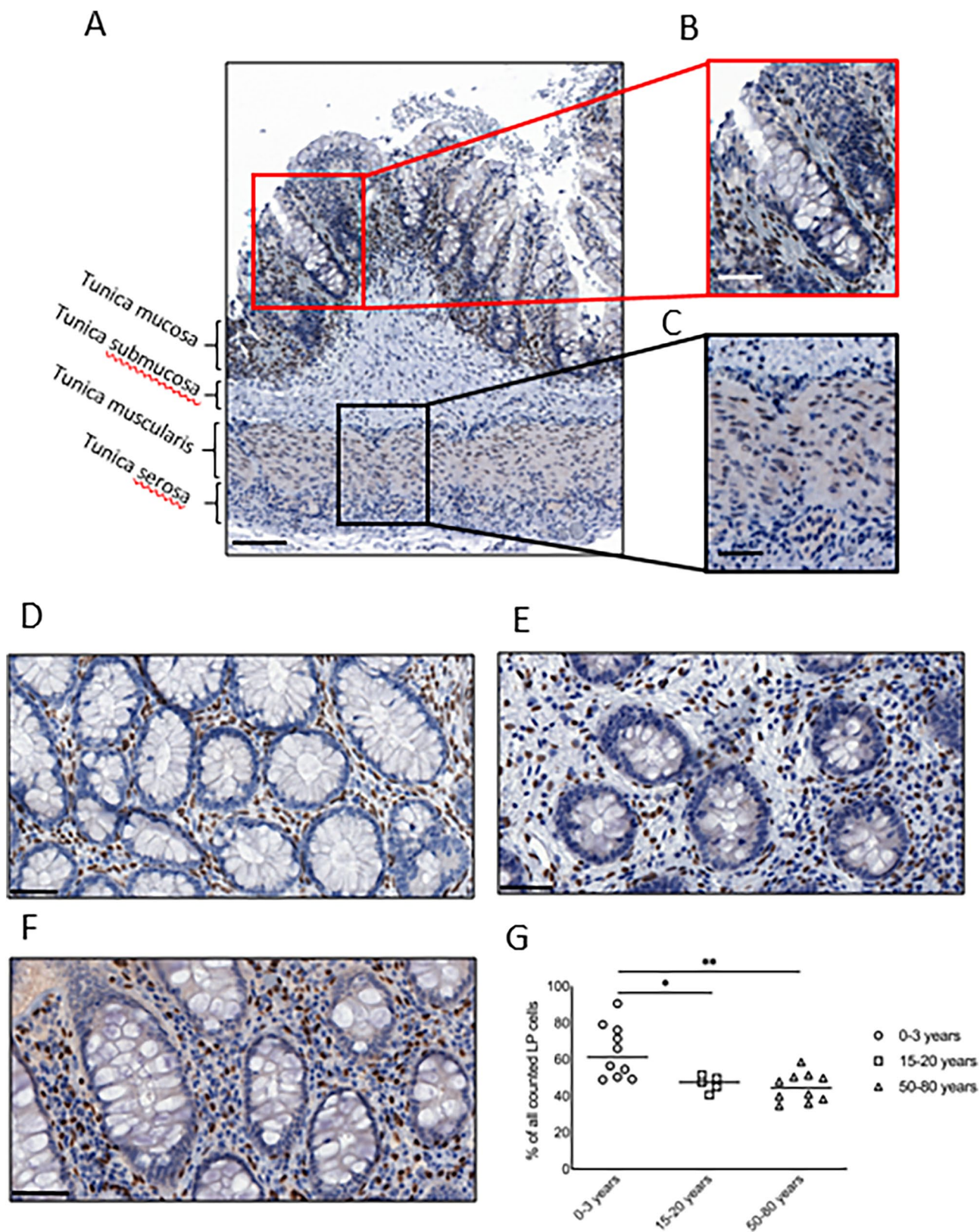


**Figure 1.** Restricted expression of NKX2-3 in the tunica mucosa and in the tunica muscularis. (A) Representative overview of NKX2-3 staining from healthy human colons. (B) Red insert from (A) showing NKX2-3 expression in the tunica mucosa. (C) Black insert from (A)

(continued)

**Figure 1. (continued)**

depicting NKX2-3 expression in the tunica muscularis. (D) Representative image showing colonic NKX2-3 expression in 0–3 years old age group. (E) Representative image showing colonic NKX2-3 expression in adolescents (15–20 years old age group). (F) Representative image showing colonic NKX2-3 expression in adults (50–80 years old age group). (G) Quantification of percentage of cells expressing NKX2-3. Scale bar in A represents 100  $\mu\text{m}$ ; in B and C, 20  $\mu\text{m}$ ; in D–F, 50  $\mu\text{m}$ . Abbreviation: LP, lamina propria. \* $p < 0.05$ , \*\* $p = 0.01$ .

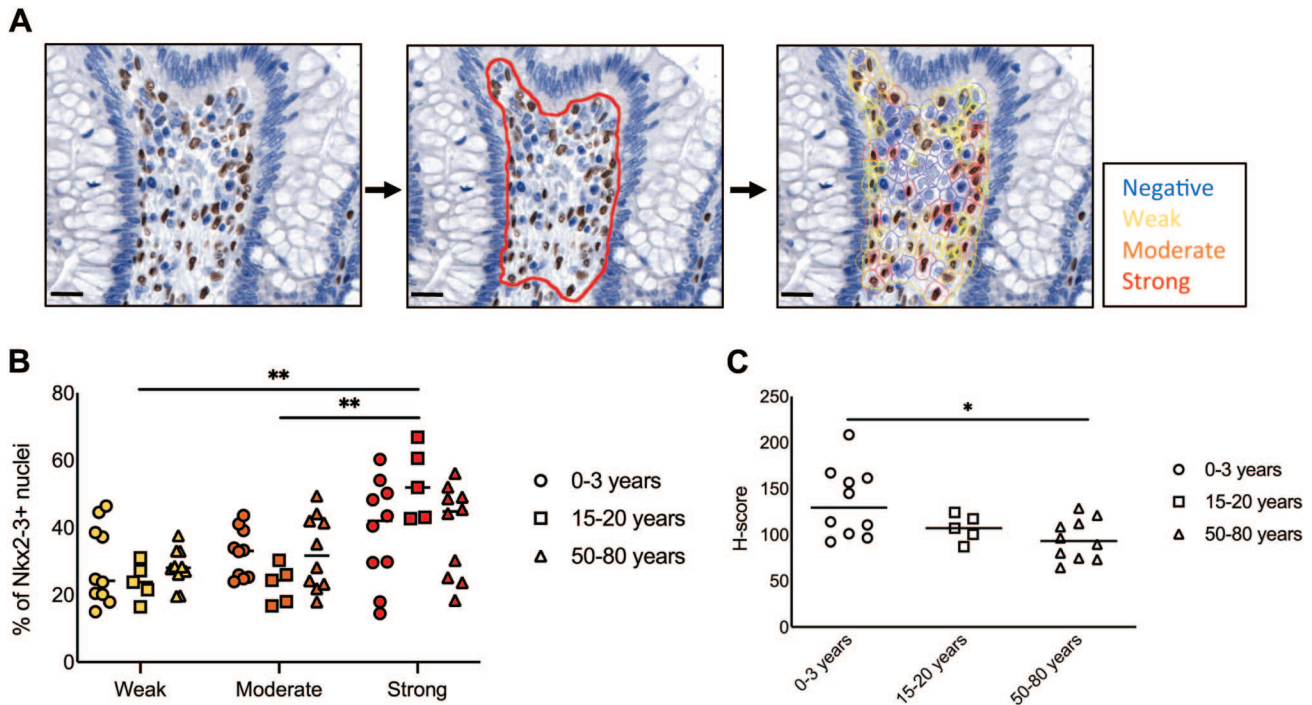


**Figure 2.** Variable staining intensities of NKX2-3 labeling during aging. (A) Representative staining illustrating the identification of cells with negative, weak, moderate, or strong NKX2-3 expression. The red line in the middle panel indicates the region analyzed. The right panel shows representative nuclei. (B) Frequencies of various staining intensities in the different age groups. Yellow, weak; orange, moderate; red, strong. (C) H-(histo)-score of NKX2-3 expression in various age groups. Scale bars, 20  $\mu\text{m}$ . \* $p < 0.05$ , \*\* $p < 0.01$ .

NKX2-3. Based on our previous dual labeling data for Factor VIII, CD34, muscle-specific actin (MSA), and  $\alpha\text{SMA}$ ,<sup>22</sup> we hypothesized that both endothelial and a substantial fraction of non-endothelial mesenchymal cells may share NKX2-3 production. In mice, a gp38<sup>+</sup> pericryptal mesenchymal stromal subset also expresses CD34, in addition to endothelial cells.<sup>33</sup> For a more detailed characterization of NKX2-3-positive mesenchymal cells in human colonic samples, we investigated the presence of NKX2-3 in subepithelial myofibroblasts that were previously found to express  $\alpha\text{SMA}$ .<sup>34</sup> Therefore, we next aimed to define the lineage affiliation of NKX2-3 expression in the pericryptal rim of the lamina propria. Due to the stronger staining of NKX2-3, we used samples from healthy 0–3 years age group for the lineage analysis.

First, corroborating our previous observations, we found that  $\alpha\text{SMA}$  is expressed in the colonic pericryptal rim, in addition to its expression in the deeper regions of the lamina propria (Fig. 3A) and the smooth muscle; however, its blurred staining pattern hampered the precise identification of the pericryptal region adjacent to the epithelium.

To study the organization of this region in further details, we used other mesenchymal markers. We found individual CD34<sup>+</sup> pericryptal cells co-expressing NKX2-3. Careful analysis indicated that these non-vascular CD34<sup>+</sup> cells could be resolved into NKX2-3-positive and NKX2-3-negative subsets (Fig. 3B), sometimes even represented by two neighboring cells. Morphometric analysis revealed that only 22.4% (234 out of 1045) of Nkx2-3-positive pericryptal cells expressed CD34. In a reverse fashion, 75% of CD34-positive cells (234 of 312) in this region displayed NKX2-3, while the remaining 25% of CD34<sup>+</sup> cells (78 out of 312) were NKX2-3-negative (Fig. 3C); in addition, CD45<sup>+</sup> leukocytes also lacked NKX2-3 expression (Fig. 3D).

In mice, vascular adhesion protein-1 (VAP-1/AOC3) has been reported to identify Nkx2-3<sup>+</sup> pericryptal myofibroblasts,<sup>30</sup> while in healthy human colon, it is also expressed in the vasculature of lamina propria and submucosa (in addition to the smooth muscle cells of the lamina muscularis mucosae), thus prompting the analysis of its correlation with NKX2-3. In the pericryptal regions, we could observe NKX2-3/VAP-1

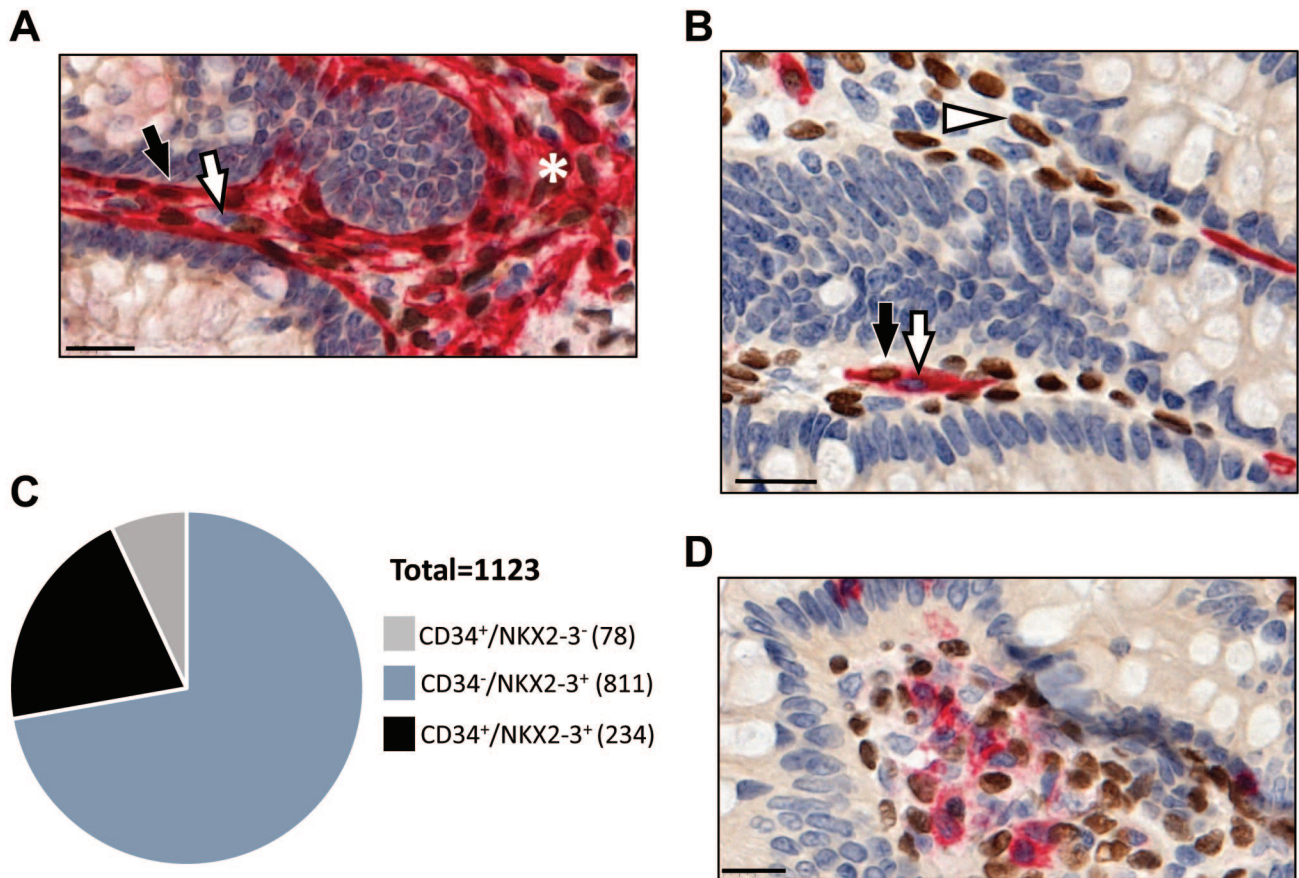


**Figure 3.** Heterogeneous expression of NKX2-3 in CD34-positive colonic pericryptal cells. (A) Representative image showing dual immunohistochemical labeling for NKX2-3 (brown) and  $\alpha$ SMA (red) ( $n=3$ ). Black and white arrows indicate double positive cells and  $\alpha$ SMA single positive cells, respectively, in the pericryptal rim. Asterisk labels lamina propria mesenchymal cell cluster. (B) Representative image of dual immunohistochemical labeling for NKX2-3 (brown) and CD34 (red) demonstrating partial overlap between the two markers ( $n=2$ ). Black arrow indicates double positive, white arrow indicates single CD34 positive, and white arrowhead indicates single NKX2-3 positive cells. (C) Quantification of the overlap between NKX2-3 expression and CD34 labeling in pericryptal cells ( $n=2$  patients). (D) CD45-positive (red) leukocytes lack NKX2-3. Scale bar, 20  $\mu$ m. Abbreviation:  $\alpha$ SMA, alpha smooth muscle antigen.

double-positive cells (Fig. 4A). Furthermore, in the deeper regions of lamina propria, we also found vascular endothelial labeling of VAP-1 (Fig. 4A). In the pericryptal zone, the majority of local VAP-1-positive cells also expressed NKX2-3 (Fig. 4B), and the comparison of the degree of overlap in NKX2-3/VAP-1 to that of NKX2-3/CD34 revealed that a larger fraction of NKX2-3-positive cells displayed VAP-1 (340 out of 669, 50.8%, Fig. 4B) than those expressing CD34 (Fig. 3C). A statistical comparison indicated that VAP-1 expression is more closely related to the production of NKX2-3 than CD34, as only 5.1% of VAP-1-positive cells (21 out of 361) lack NKX2-3 labeling, while as shown earlier, 25% of CD34<sup>+</sup> lacked NKX2-3 (Fig. 4C,  $p<0.0001$ ).

To identify NKX2-3-positive lamina propria mesenchymal cells lacking all these endothelial/myofibroblastic

markers, we next performed dual labeling with a cocktail of anti-CD34/VAP-1/ $\alpha$ SMA antibodies visualized with the same red precipitate and correlating it with NKX2-3 detection via brown DAB chromogen. We found that although the majority of NKX2-3<sup>+</sup> cells also stained positive with the anti-CD34/VAP-1/ $\alpha$ SMA cocktail, NKX2-3 single positive cells were still readily detectable (Fig. 4D). Similar to the extensive labeling observed for evaluation of  $\alpha$ SMA staining, our attempts to quantify the overlap with NKX2-3 staining were futile. Taken together, our results reveal that, although the majority of histologically detectable NKX2-3<sup>+</sup> cells can be assigned to various pericryptal myofibroblast lineages, none of the markers employed appears to be able to uniquely identify the NKX2-3<sup>+</sup> cells; in addition, a small fraction of NKX2-3<sup>+</sup> cells do not display CD34, VAP-1, or  $\alpha$ SMA.

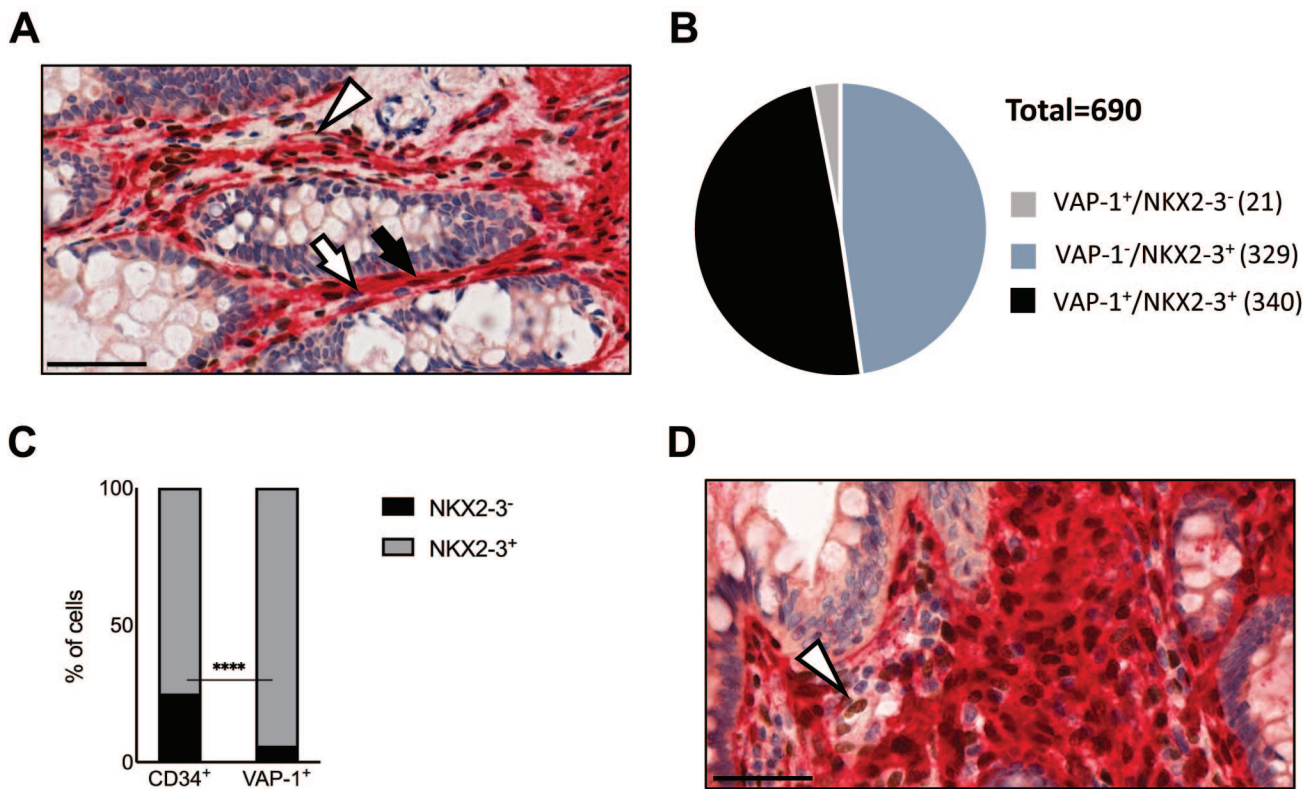


**Figure 4.** Heterogeneous expression of NKX2-3 in VAP-1-positive colonic pericryptal mesenchymal cells. (A) Representative images showing dual immunohistochemical labeling for NKX2-3 (brown) and VAP-1 (red) ( $n=3$ ). Black arrow and white arrows indicate pericryptal double positive cells and VAP-1 single positive cells, respectively; arrowhead points to a capillary lined by VAP-1-positive endothelial cells. (B) Quantification of the overlap between NKX2-3 expression and VAP-1 labeling in pericryptal cells. The measurement was carried out at the distance of less than 20  $\mu\text{m}$  from the crypt edge ( $n=2$  patients). (C) Quantification of NKX2-3<sup>+</sup> (gray) or NKX2-3<sup>-</sup> cells among CD34<sup>+</sup> cells (left) and VAP-1<sup>+</sup> cells (right). (D) A representative image of staining with Nkx2-3 (brown) and CD34/ $\alpha$ SMA/VAP-1 (red) ( $n=2$ ). White arrowhead indicates an NKX2-3 single positive cell. Scale bar, 50  $\mu\text{m}$ . Abbreviations:  $\alpha$ SMA, alpha smooth muscle antigen; VAP-1, vascular adhesion protein-1.

### Distribution and Ratio of NKX2-3<sup>+</sup> Cells in Colorectal Cancer Samples

Previous reports identified polymorphisms in NKX2-3 as a susceptibility trait associated with inflammatory bowel diseases,<sup>35</sup> and its absence in mice resulted in enhanced epithelial proliferation in both homeostatic and inflammatory conditions,<sup>29</sup> thus raising its potential involvement in epithelial proliferative conditions, including polyps and adenocarcinomas. Therefore, next we examined the expression of NKX2-3 in patients with either pre-malignant adenomatous polyps or malignant adenocarcinomas (Table 1). The cohort of normal 50- to 80-year-old samples was used as age-matched controls.

Similar to non-tumor samples, NKX2-3<sup>+</sup> cells were homogeneously distributed throughout the lamina propria of polyp and adenocarcinoma samples (Fig. 5A and B). Comparing the frequency of NKX2-3<sup>+</sup> nuclei relative to the total number of nuclei, we observed a lower percentage in polyps than in non-tumor controls ( $p=0.0433$ ), and this frequency further decreased ( $p=0.0003$ ) in

adenocarcinoma samples (Fig. 5C). On the other hand, the difference between polyp and adenocarcinoma samples did not reach statistical significance.

To dissect whether the reduction of NKX2-3-positive nuclei is a general phenomenon or is related to a shift in labeling intensity, we analyzed the distribution of nuclei with various NKX2-3 expression levels. In general, we found that in both polyp and adenocarcinoma samples, weakly labeled NKX2-3<sup>+</sup> cells represented the largest proportion of nuclei (Fig. 5D). The percentage of these cells was significantly increased compared to healthy controls, coupled with significant decreases in the moderately and strongly NKX2-3<sup>+</sup> nuclei. This was in contrast to the findings in healthy controls where intensely NKX2-3<sup>+</sup> cells represented the largest fraction of cells.

In line with the reduced number and labeling intensity of NKX2-3-positive nuclei, we also observed a significantly lower H-score in both polyp and CRC samples than those in healthy samples (Fig. 5E;  $p=0.0288$  and  $p<0.0001$ , respectively). Moreover, in



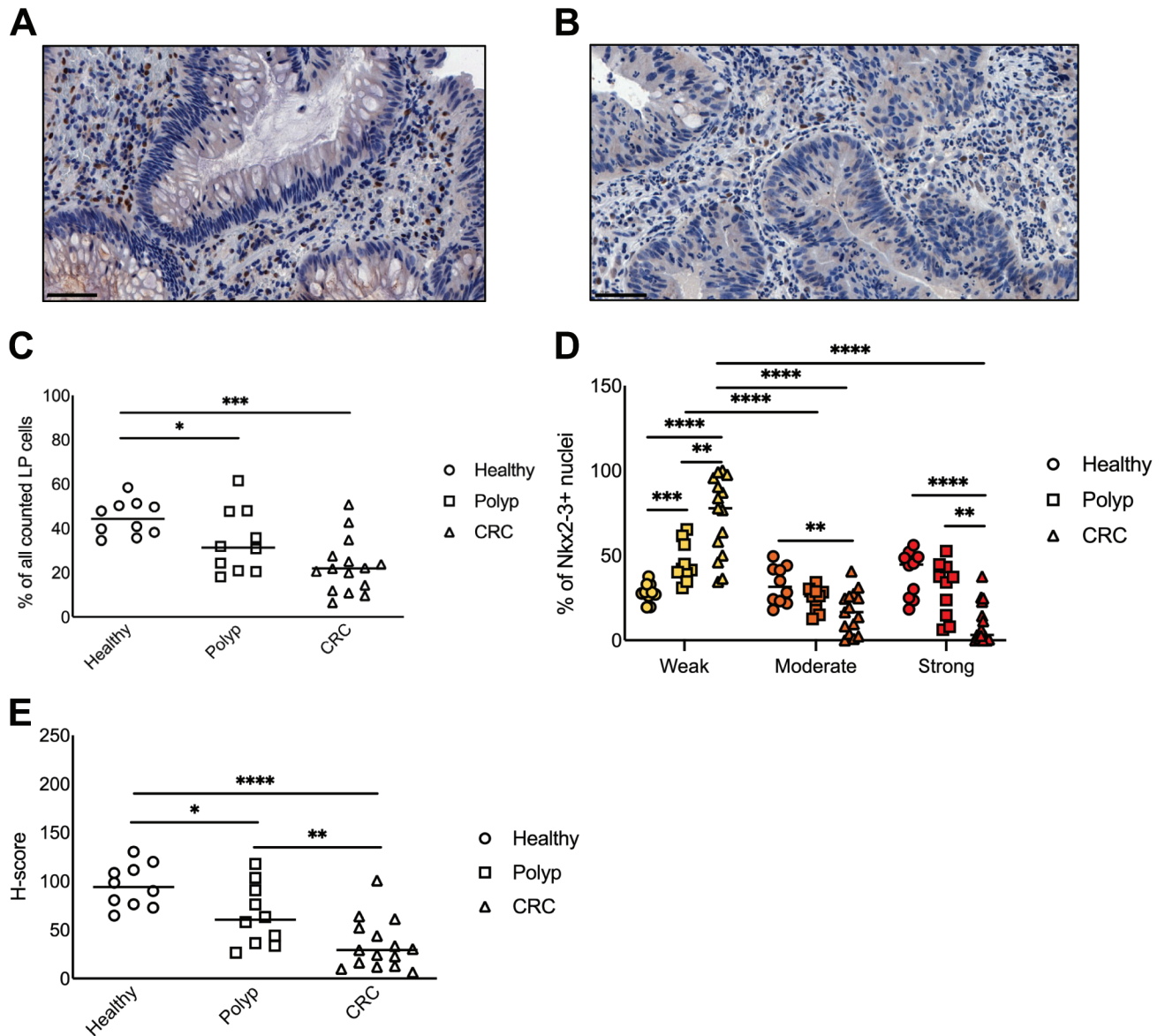


**Figure 5.** Decreased expression of NKX2-3 in pre-malignant and malignant colon tissues. (A) Representative image showing NKX2-3 expression in colonic polyps. (B) Representative image showing NKX2-3 expression in colon adenocarcinoma samples. (C) Frequencies of NKX2-3<sup>+</sup> cells in non-tumor, polyp, and adenocarcinoma samples. (D) Frequencies of weak, intermediate, and strong NKX2-3<sup>+</sup> cells in non-tumor, polyp, and adenocarcinoma samples. Yellow, weak; orange, moderate; red, strong. (E) H-score of non-tumor, polyp, and adenocarcinoma samples. Scale bar in (A) and (B) represents 50  $\mu$ m. Abbreviations: CRC, colorectal carcinoma, LP, lamina propria. \* $p < 0.05$ , \*\* $p < 0.01$ , \*\*\* $p < 0.001$ , \*\*\*\* $p < 0.0001$ .

CRC samples, the H-score was significantly lower ( $p = 0.0096$ ) than that in polyp samples.

Taken together, these findings establish the loss of cells with strong NKX2-3 expression in patients with adenomatous polyp or with defined colonic adenocarcinoma.

## Discussion

In our present work, we studied the presence and distribution of the NKX2-3 homeodomain transcription

factor in humans to define its course of expression during aging and in colorectal malignancies. Our findings demonstrate a heterogeneous expression pattern shared between various endothelial as well as fibroblastic cell subsets and differential production affected by both aging and malignant transformation.

First, we investigated the colonic expression pattern of NKX2-3 at various ages from histologically normal samples. Our findings reveal a more pronounced expression in the youngest age group, probably reflecting the organ growth in this period.

The bulk of reactivity was observed in the subepithelial region of the colonic lamina propria, where a shared co-expression with mesenchymal stromal markers was detected, including CD34,  $\alpha$ SMA, and VAP-1.

The endothelial expression of NKX2-3 may be needed for the maintenance of capillary organization, as its inherited mutation has been demonstrated to be associated with intestinal varices.<sup>24</sup> Furthermore, the inhibition of NKX2-3 in ileal microvascular endothelial cells *in vitro* led to the reduction of mRNA expression of Mucosal addressin cell adhesion molecule-1 (MAdCAM-1), AKR thymoma kinase (AKT), and Vascular cell adhesion molecule (VCAM1) surface molecules.<sup>36</sup> These observations indicate endothelial effects as well as possible communication (membrane-associated or soluble) with other cells, including leukocytes that can contribute to the hitherto unexplored relationship between altered expression of NKX2-3 and inflammatory bowel diseases.<sup>35</sup> The endothelial effects of Nkx2-3 in murine PPs HEVs involve the transcriptional action of a composite recognition element in the regulatory regions for Nkx2-3 and COUP-TFII proteins, influencing the expression of MAdCAM-1 addressin and St6Gal1 sulfotransferase enzyme defining the addressin's glycosylation characteristics.<sup>37</sup> While Nkx2-3 is also expressed in hematopoietic stem cells (HSCs) influencing their homeostasis, in mature leukocytes, Nkx2-3 is absent, in agreement with our immunohistochemical observations in human samples. Although the absence of Nkx2-3 in mice causes defective development of PPs and isolated follicles and suppresses dextran sulfate sodium (DSS)-induced colitis,<sup>25,26,29</sup> this deviation is likely to be related to disrupted endothelial specification affecting intestinal immunity.

While the (venous) endothelial expression of NKX2-3 may contribute to leukocyte homing to the intestines and inflammatory responses, the non-endothelial production of NKX2-3 within the lamina propria may be more closely related to the differentiation of colonic epithelial cells, via establishing the colonic niche for intestinal epithelial stem cells (IESCs) expressing Lgr5.<sup>5,30</sup> In our subsequent analyses aimed at defining the lineage affiliation of NKX2-3-positive colonic stromal cells, we consistently found that the colonic epithelial cells themselves do not express detectable amounts of NKX2-3 protein; on the other hand, a significant fraction of the non-endothelial lamina propria stromal cells expressing CD34,  $\alpha$ SMA, and/or VAP-1 produce NKX2-3. This arrangement is similar to that in mice, where the proximity of Lgr5<sup>+</sup> IESCs and CD34<sup>+</sup>/gp38<sup>+</sup> pericryptal mesenchymal cells producing Wnt2b, Gremlin-1, and R-spondin1 appears to be a main factor in maintaining the

homeostasis of IESCs following tissue damage and inflammation.<sup>33</sup> The differential representation of NKX2-3<sup>+</sup> cells among the VAP-1-positive and CD34-positive pericryptal compartments, together with the difference between the total NKX2-3-positive nuclei and the sum of VAP-1 and CD34 expression, suggests both a partial overlap for VAP-1 and CD34 (thus the likely existence of VAP-1<sup>+</sup>/CD34<sup>-</sup> cells) and the presence of VAP-1<sup>-</sup>/CD34<sup>-</sup> cells among the pericryptal NKX2-3-positive cells. To clarify the distribution of these presumed stromal subsets, the combination of CD31 and CD34 with VAP-1 as surface markers correlated with NKX2-3 expression may offer a possible approach to identify putative intestinal myofibroblastic cells for further analyses, including their support functions for epithelial differentiation of IESCs. This approach may also confirm the existence of a putative "triple negative" (i.e. CD34/VAP-1/ $\alpha$ SMA-negative) NKX2-3-positive subset demonstrated in our combined immunohistochemical labeling that we assume as a minor population.

Our immunohistochemical results demonstrating the lack of clear lineage-restricted expression of NKX2-3 is in line with recent scRNAseq analyses revealing a wide range of mesenchymal cells transcribing NKX2-3, including (but not limited to) myofibroblasts, ADAMDEC<sup>+</sup> stromal cells, CCL11<sup>+</sup> stromal cells, CH25H<sup>+</sup> stromal cells, and others<sup>16</sup> ([www.gutcellatlas.org](http://www.gutcellatlas.org)). Within the endothelial compartment, NKX2-3 was transcribed in cycling (Ki67<sup>+</sup>) endothelial cells and capillary endothelium, but not in lymphatic endothelium. Importantly, in this database, NKX2-3 was absent from epithelial cells and hematopoietic cells, similar to our histological results.

Finally, in our immunohistochemical analysis of NKX2-3 expression in polyps and CRC samples, we found that NKX2-3 is downregulated in the connective tissue. This raises the question whether the expansion of cancer cells may alter the transcriptional profile of cancer-associated fibroblasts (CAFs), or the initial reduction of NKX2-3 may create a permissive environment for the emergence of CRC. CAFs contribute to the expansion of carcinoma cells in several ways, and their unequivocal identification is hampered by the lack of universal markers and phenotype. Initially, CAFs may emerge from local fibroblasts; however, at later stages, epithelial as well as pericytes, endothelial cells, and mesenchymal stem cells may also give rise to CAFs.<sup>38</sup> The observed reduction of NKX2-3 suggests either reduced production by the resident stromal cells or their partial replacement by cells originally lacking NKX2-3 production. Although the effect of differential NKX2-3 mRNA and protein expression between various colonic and/or rectal segments cannot be excluded, previous

data reporting NKX2.3 expression in a Gene Expression Omnibus data set involving cancer and normal mucosa samples from the colon do not reveal significant differences when normal mucosa from left and right colon are compared (GSE44076; <https://www.ncbi.nlm.nih.gov/geo/query/acc.cgi?acc=GSE44076>); however, expression is significantly reduced in cancer compared to normal mucosa. Our earlier findings on the enhanced epithelial proliferation and intestinal regeneration in mice lacking Nkx2-3 in DSS-induced colitis model<sup>29</sup> can be reconciled with the negative relationship between NKX2-3 expression and epithelial cell expansion in human colon. It remains to be investigated whether the lack of Nkx2-3 enhances the propensity for colorectal cancers in these mice. As suggested earlier, exploiting the possible combination of CD31 (to specify endothelial cells) with CD34 and VAP-1 (as shared endothelial/mesenchymal markers) for cell sorting may also provide further data on the altered production of NKX2-3 between normal and CRC or polyp samples from humans. It is yet unknown whether various CRC-associated mutations (KRAS, NRAS, and BRAF)<sup>39</sup> or fibroblast activation protein (FAP) production<sup>40</sup> may modify or correlate with the expression of NKX2-3. In addition, follow-up studies of samples taken from various stages of cancer progression and therapeutic response and larger cohort may further pinpoint differential representation of the FAP-positive CAF compartment with various degrees of NKX2-3 expression. As the expression of NKX2-3 in the non-invasive adenomatous polyps (with preserved stromal composition) is already reduced, it is likely that the downregulation of NKX2-3 is associated with creating a permissive condition for subsequent transformation and malignant expansion of cancer cells in CRC. Further studies with lineage-specific targeted inactivation of Nkx2-3 in mice may provide important clues on the role of this mesenchymal transcription factor in the propagation of epithelium-derived colonic malignancies.

### Acknowledgments

The authors gratefully acknowledge the expert contribution of Ms. Judit Szilágyiné in optimizing and performing immunohistochemical protocols. The authors wish to thank Dr. Giovanna Roncador (Monoclonal Antibodies Unit, Spanish National Cancer Research Center, Madrid, Spain) for generously providing the rat anti-human NKX2-3 monoclonal antibody.

### Competing Interests

The author(s) declared no potential conflicts of interest with respect to the research, authorship, and/or publication of this article.


### Author Contributions

Z.K. and P.B. conceived the study plan, evaluated the results, and wrote the manuscript. F.G. contributed to the immunohistochemical staining and performed morphometric analyses and statistical evaluation. B.K. selected the tissue samples and evaluated their histological characteristics. P.B. secured research funding. F.G. and B.K. are equal first authors. Z.K. and P.B. are equal last authors.

### Funding

The author(s) disclosed receipt of the following financial support for the research, authorship, and/or publication of this article: P.B. is supported by the Hungarian Science Foundation NKFI grant no. 128322, GINOP 2.3.2-15-2016-00022, 2020-4.1.1-TKP2020, TKP2021-EGA-10, and EFOP-3.6.1-16.2016.00004 EU funds. This project was supported by the János Bolyai Research Scholarship of the Hungarian Academy of Sciences (to Z.K.) and the ÚNKP-22-5 New National Excellence Program of the Ministry for Culture and Innovation from the source of the National Research, Development, and Innovation Fund (to Z.K.).

### ORCID iDs

Fanni Gábris  <https://orcid.org/0000-0002-6036-3941>

Béla Kajtár  <https://orcid.org/0000-0001-5551-3709>

Péter Balogh  <https://orcid.org/0000-0001-5749-4775>

### Literature Cited

1. Bos A, van Egmond M, Mebius R. The role of retinoic acid in the production of immunoglobulin A. *Mucosal Immunol.* 2022;15(4):562–72. doi:10.1038/s41385-022-00509-8
2. Larange A, Cheroutre H. Retinoic acid and retinoic acid receptors as pleiotropic modulators of the immune system. *Annu Rev Immunol.* 2016;34:369–94. doi:10.1146/annurev-immunol-041015-055427
3. Peterson LW, Artis D. Intestinal epithelial cells: regulators of barrier function and immune homeostasis. *Nat Rev Immunol.* 2014;14(3):141–53. doi:10.1038/nri3608
4. Qiu J, Ma Y, Qiu J. Regulation of intestinal immunity by dietary fatty acids. *Mucosal Immunol.* 2022;15(5):846–56. doi:10.1038/s41385-022-00547-2
5. Barker N, van Es JH, Kuipers J, Kujala P, van den Born M, Cozijnsen M, Haegebarth A, Korving J, Begthel H, Peters PJ, Clevers H. Identification of stem cells in small intestine and colon by marker gene Lgr5. *Nature.* 2007;449(7165):1003–7. doi:10.1038/nature06196
6. Kiefer JC. Molecular mechanisms of early gut organogenesis: a primer on development of the digestive tract. *Dev Dyn.* 2003;228(2):287–91. doi:10.1002/dvdy.10382
7. Chevalier NR. Physical organogenesis of the gut. *Development.* 2022;149(16):dev200765. doi:10.1242/dev.200765
8. Madison BB, Braunstein K, Kuizon E, Portman K, Qiao XT, Gumucio DL. Epithelial hedgehog signals

- pattern the intestinal crypt-villus axis. *Development*. 2005;132(2):279–89. doi:10.1242/dev.01576
9. Walton KD, Kolterud A, Czerwinski MJ, Bell MJ, Prakash A, Kushwaha J, Grosse AS, Schnell S, Gumucio DL. Hedgehog-responsive mesenchymal clusters direct patterning and emergence of intestinal villi. *Proc Natl Acad Sci U S A*. 2012;109(39):15817–22. doi:10.1073/pnas.1205669109
  10. Furness JB. The enteric nervous system and neurogastroenterology. *Nat Rev Gastroenterol Hepatol*. 2012;9(5):286–94. doi:10.1038/nrgastro.2012.32
  11. Sharkey KA, Mawe GM. The enteric nervous system. *Physiol Rev*. 2023;103(2):1487–564. doi:10.1152/physrev.00018.2022
  12. Progotzky F, Pachnis V. The role of enteric glia in intestinal immunity. *Curr Opin Immunol*. 2022;77:102183. doi:10.1016/j.coi.2022.102183
  13. Finke D, Meier D. Molecular networks orchestrating GALT development. *Curr Top Microbiol Immunol*. 2006;308:19–57. doi:10.1007/3-540-30657-9\_2
  14. Kanamori Y, Ishimaru K, Nanno M, Maki K, Ikuta K, Nariuchi H, Ishikawa H. Identification of novel lymphoid tissues in murine intestinal mucosa where clusters of c-kit<sup>+</sup> IL-7R<sup>+</sup> Thy1<sup>+</sup> lympho-hemopoietic progenitors develop. *J Exp Med*. 1996;184(4):1449–59. doi:10.1084/jem.184.4.1449
  15. Mörbe UM, Jørgensen PB, Fenton TM, von Burg N, Riis LB, Spencer J, Agace WW. Human gut-associated lymphoid tissues (GALT); diversity, structure, and function. *Mucosal Immunol*. 2021;14(4):793–802. doi:10.1038/s41385-021-00389-4
  16. Elmentaite R, Kumasaka N, Roberts K, Fleming A, Dann E, King HW, Kleshchevnikov V, Dabrowska M, Pritchard S, Bolt L, Vieira SF, Mamanova L, Huang N, Perrone F, Goh Kai'En I, Lisgo SN, Katan M, Leonard S, Oliver TRW, Hook CE, Nayak K, Campos LS, Domínguez Conde C, Stephenson E, Engelbert J, Botting RA, Polanski K, van Dongen S, Patel M, Morgan MD, Marioni JC, Bayraktar OA, Meyer KB, He X, Barker RA, Uhlig HH, Mahbubani KT, Saeb-Parsy K, Zilbauer M, Clatworthy MR, Haniffa M, James KR, Teichmann SA. Cells of the human intestinal tract mapped across space and time. *Nature*. 2021;597(7875):250–5. doi:10.1038/s41586-021-03852-1
  17. Fawkner-Corbett D, Antanaviciute A, Parikh K, Jagielowicz M, Gerós AS, Gupta T, Ashley N, Khamis D, Fowler D, Morrissey E, Cunningham C, Johnson PRV, Koohy H, Simmons A. Spatiotemporal analysis of human intestinal development at single-cell resolution. *Cell*. 2021;184(3):810–26.e23. doi:10.1016/j.cell.2020.12.016
  18. Hickey JW, Becker WR, Nevins SA, Horning A, Perez AE, Zhu C, Zhu B, Wei B, Chiu R, Chen DC, Cotter DL, Esplin ED, Weimer AK, Caraccio C, Venkataramanan V, Schürch CM, Black S, Brbić M, Cao K, Chen S, Zhang W, Monte E, Zhang NR, Ma Z, Leskovec J, Zhang Z, Lin S, Longacre T, Plevritis SK, Lin Y, Nolan GP, Greenleaf WJ, Snyder M. Organization of the human intestine at single-cell resolution. *Nature*. 2023;619(7970):572–84. doi:10.1038/s41586-023-05915-x
  19. Beck F. Homeobox genes in gut development. *Gut*. 2002;51(3):450–4. doi:10.1136/gut.51.3.450
  20. Heath JK. Transcriptional networks and signaling pathways that govern vertebrate intestinal development. *Curr Top Dev Biol*. 2010;90:159–92. doi:10.1016/s0070-2153(10)90004-5
  21. Stanfel MN, Moses KA, Schwartz RJ, Zimmer WE. Regulation of organ development by the NKX-homeodomain factors: an NKX code. *Cell Mol Biol*. 2005;Suppl 51:OL785–99.
  22. Vojkovic D, Kellermayer Z, Kajtár B, Roncador G, Vincze Á, Balogh P. Nkx2-3—a slippery slope from development through inflammation toward hematopoietic malignancies. *Biomark Insights*. 2018;13. doi:10.1177/1177271918757480
  23. Leon TY, Ngan ES, Poon HC, So MT, Lui VC, Tam PK, Garcia-Barcelo MM. Transcriptional regulation of RET by Nkx2-1, Phox2b, Sox10, and Pax3. *J Pediatr Surg*. 2009;44(10):1904–12. doi:10.1016/j.jpedsurg.2008.11.055
  24. Kerkhofs C, Stevens SJC, Faust SN, Rae W, Williams AP, Wurm P, Østern R, Fockens P, Würfel C, Laass M, Kokke F, Stegmann APA, Brunner HG. Mutations in RPSA and NKX2-3 link development of the spleen and intestinal vasculature. *Hum Mutat*. 2020;41(1):196–202. doi:10.1002/humu.23909
  25. Pabst O, Förster R, Lipp M, Engel H, Arnold HH. NKX2.3 is required for MAdCAM-1 expression and homing of lymphocytes in spleen and mucosa-associated lymphoid tissue. *Embo J*. 2000 May 2;19(9):2015–23. doi:10.1093/emboj/19.9.2015
  26. Wang CC, Biben C, Robb L, Nassir F, Barnett L, Davidson NO, Koentgen F, Tarlinton D, Harvey RP. Homeodomain factor Nkx2-3 controls regional expression of leukocyte homing coreceptor MAdCAM-1 in specialized endothelial cells of the viscera. *Dev Biol*. 2000;224(2):152–67. doi:10.1006/dbio.2000.9749
  27. Kellermayer Z, Mihalj M, Lábadi Á, Czömpöly T, Lee M, O'Hara E, Butcher EC, Berta G, Balogh A, Arnold HH, Balogh P. Absence of Nkx2-3 homeodomain transcription factor reprograms the endothelial addressin preference for lymphocyte homing in Peyer's patches. *J Immunol*. 2014;193(10):5284–93. doi:10.4049/jimmunol.1402016
  28. Vojkovic D, Kellermayer Z, Gábris F, Schippers A, Wagner N, Berta G, Farkas K, Balogh P. Differential effects of the absence of Nkx2-3 and MAdCAM-1 on the distribution of intestinal type 3 innate lymphoid cells and postnatal SILT formation in mice. *Front Immunol*. 2019;10:366. doi:10.3389/fimmu.2019.00366
  29. Kellermayer Z, Vojkovic D, Dakah TA, Bodó K, Botz B, Helyes Z, Berta G, Kajtár B, Schippers A, Wagner N, Scotto L, O'Connor OA, Arnold HH, Balogh P. IL-22-independent protection from colitis in the absence of Nkx2.3 transcription factor in mice. *J Immunol*. 2019;202(6):1833–44. doi:10.4049/jimmunol.1801117

30. Hsia LT, Ashley N, Ouaret D, Wang LM, Wilding J, Bodmer WF. Myofibroblasts are distinguished from activated skin fibroblasts by the expression of AOC3 and other associated markers. *Proc Natl Acad Sci U S A*. 2016;113(15):E2162–71. doi:10.1073/pnas.1603534113
31. Pabst O, Schneider A, Brand T, Arnold HH. The mouse *Nkx2-3* homeodomain gene is expressed in gut mesenchyme during pre- and postnatal mouse development. *Dev Dyn*. 1997;209(1):29–35. doi:10.1002/(sici)1097-0177(199705)209:1<29::Aid-aja3>3.0.Co;2-z
32. Robles EF, Mena-Varas M, Barrio L, Merino-Cortes SV, Balogh P, Du MQ, Akasaka T, Parker A, Roa S, Panizo C, Martin-Guerrero I, Siebert R, Segura V, Agirre X, Macri-Pellizeri L, Aldaz B, Vilas-Zornoza A, Zhang S, Moody S, Calasanz MJ, Tousseyn T, Broccardo C, Brousset P, Campos-Sanchez E, Cobaleda C, Sanchez-Garcia I, Fernandez-Luna JL, Garcia-Muñoz R, Pena E, Bellosillo B, Salar A, Baptista MJ, Hernandez-Rivas JM, Gonzalez M, Terol MJ, Climent J, Ferrandez A, Sagaert X, Melnick AM, Prosper F, Oscier DG, Carrasco YR, Dyer MJ, Martinez-Climent JA. Homeobox NKX2-3 promotes marginal-zone lymphomagenesis by activating B-cell receptor signalling and shaping lymphocyte dynamics. *Nat Commun*. 2016;7:11889. doi:10.1038/ncomms11889
33. Stzepourginski I, Nigro G, Jacob JM, Dulauroy S, Sansonetti PJ, Eberl G, Peduto L. CD34+ mesenchymal cells are a major component of the intestinal stem cells niche at homeostasis and after injury. *Proc Natl Acad Sci U S A*. 2017;114(4):E506–13. doi:10.1073/pnas.1620059114
34. Adegboyega PA, Mifflin RC, DiMari JF, Saada JI, Powell DW. Immunohistochemical study of myofibroblasts in normal colonic mucosa, hyperplastic polyps, and adenomatous colorectal polyps. *Arch Pathol Lab Med*. 2002;126(7):829–36. doi:10.5858/2002-126-0829-isomin
35. Parkes M, Barrett JC, Prescott NJ, Tremelling M, Anderson CA, Fisher SA, Roberts RG, Nimmo ER, Cummings FR, Soars D, Drummond H, Lees CW, Khawaja SA, Bagnall R, Burke DA, Todhunter CE, Ahmad T, Onnie CM, McArdle W, Strachan D, Bethel G, Bryan C, Lewis CM, Deloukas P, Forbes A, Sanderson J, Jewell DP, Satsangi J, Mansfield JC, Cardon L, Mathew CG. Sequence variants in the autophagy gene IRGM and multiple other replicating loci contribute to Crohn's disease susceptibility. *Nat Genet*. 2007;39(7):830–2. doi:10.1038/ng2061
36. Yu W, Hegarty JP, Berg A, Chen X, West G, Kelly AA, Wang Y, Poritz LS, Koltun WA, Lin Z. NKX2-3 transcriptional regulation of endothelin-1 and VEGF signaling in human intestinal microvascular endothelial cells. *PLoS One*. 2011;6(5):e20454. doi:10.1371/journal.pone.0020454
37. Dinh TT, Xiang M, Rajaraman A, Wang Y, Salazar N, Zhu Y, Roper W, Rhee S, Brulois K, O'Hara E, Kiefel H, Dinh TM, Bi Y, Gonzalez D, Bao EP, Red-Horse K, Balogh P, Gábris F, Gaszner B, Berta G, Pan J, Butcher EC. An NKX-COUP-TFII morphogenetic code directs mucosal endothelial addressin expression. *Nat Commun*. 2022;13(1):7448. doi:10.1038/s41467-022-34991-2
38. Sahai E, Astsaturov I, Cukierman E, DeNardo DG, Egeblad M, Evans RM, Fearon D, Greten FR, Hingorani SR, Hunter T, Hynes RO, Jain RK, Janowitz T, Jorgensen C, Kimmelman AC, Kolonin MG, Maki RG, Powers RS, Puré E, Ramirez DC, Scherz-Shouval R, Sherman MH, Stewart S, Tlsty TD, Tuveson DA, Watt FM, Weaver V, Weeraratna AT, Werb Z. A framework for advancing our understanding of cancer-associated fibroblasts. *Nat Rev Cancer*. 2020;20(3):174–86. doi:10.1038/s41568-019-0238-1
39. Bożyk A, Krawczyk P, Reszka K, Krukowska K, Kolak A, Mańdziuk S, Wojas-Krawczyk K, Ramlau R, Milanowski J. Correlation between. *Arch Med Sci*. 2022;18(5):1221–30. doi:10.5114/aoms/109170
40. Kalaei Z, Manafi-Farid R, Rashidi B, Kiani FK, Zarei A, Fathi M, Jadidi-Niaragh F. The Prognostic and therapeutic value and clinical implications of fibroblast activation protein- $\alpha$  as a novel biomarker in colorectal cancer. *Cell Commun Signal*. 2023;21(1):139. doi:10.1186/s12964-023-01151-y

